Modeling of Variable Speed Wind Turbines with Doubly Fed Induction Generator for Studying Steady State Operation

نمذجة تربينات الرياح متغيرة السرعة المرتبطة بالمولدات الإستنتاجية ثنائية التغذية لدراسة الأداء المستقر لنظم القوى

M.M. El-Saadawi[1] S. S. Kaddah[1] M. G. Osman[1]
S. A. El-Drieny[1] M. N. Abdel-Wahab[2]

[1]Dept. of EE, Faculty of Engineering, Mansoura University, Egypt
[2]Egyptian Electricity Transmission Co. EETC, Egypt

ملخص البحث :

من الضروري دراسة الأداء المستقر لمنظومة القوى الكهربية عند ربطها بمولدات تربينات الرياح. وكذلك تطوير برامج ونظم تشغيل الشبكات الكهربية للحصول على افضل أداء ممكن لهذه الشبكات للتغلب على المشاكل التى قد تنشأ عند ربط مزارع تربينات الرياح معها.

فى هذا البحث تم استنباط طريقة رياضية مرنة لنمذجة منظومة تربينات الرياح متغيرة السرعة مرتبطة بمولدات استنتاجية مزدوجة التغذية بالإضافة إلي وسائط ربطها بمنظومة القوى الكهربية عن طريق مناوب القدرة بحيث يتم دمجها ونمذجتها معاً.

كما تم تطوير برامج حاسب آلى باستخدام بيئة الماتلاب (MATLAB) لتمثيل تلك المنظومة و دراسة أدائها عند ربطها مع شبكات القوى الكهربية باستخدام تحليل تدفق القدرة الكهربية الفعالة والغير فعالة ودراسة أوجه المقارنة لكل منظومة لاختيار الأنسب توافقا مع كل شبكة كهربية فى الظروف العادية أو الطارئة.

وقد تم تنفيذ الخوارزم المقترح وتطبيقه علي نظام اختبار قياسى (IEEE 26 – BUS) و دراسة تأثير ادماج هذه التربينات على قضبان التوزيع القياسية (Reference Bus) لنظام الاختبار المقترح وتحديد العدد الأمثل للتربينات للحفاظ على الأداء العام لمنظومة القوى و تحديد أفضل مكان يتم وضعها فيه لتجنب التأثيرات العكسية على المنظومة.

Abstract

Wind energy conversion has emerged as a viable alternative to meet the increased demand for energy resources in recent years. Wind farms interconnected to power system bring new challenges to power system operation. It is imperative to study the impact of variable speed wind turbine coupled to doubly fed induction generator DFIG on utility grid operation.

A mathematical model has been developed to evaluate the steady state performance of the variable speed wind energy conversion system with DFIG. In addition a steady state converter (rectifier-inverter) model as a function of firing angles of the rectifier and inverter is developed and used directly to calculate the influence of DFIG on power system operation through power flow solution. These units are modeled as P-V bus(es) to manage the reactive power generation inside the wind farm. The paper presents and validates a model of DFIG suitable for operation in steady state mode and not only able to support voltage by feeding reactive power but also to fulfill grid requirement. The proposed algorithm is implemented and applied to the IEEE 26-bus system and the number of the equivalent wind turbines generating units WTGU at each generating bus is demonstrated and injected as P-V bus(es). The impact of WTGUs on active and reactive power of own generating bus(es) and slack bus at different wind speeds is also investigated.

Keywords: *doubly fed induction generator, renewable energy sources, wind turbine modeling, power system operation, WTGU wind turbine generating units.*

Accepted March 31, 2010.

1. Introduction

Wind Turbines (WT) operate at a fixed speed or variable speed. For fixed speed wind turbine, the squirrel cage induction generator is directly connected to the electrical grid via capacitor banks. This configuration enables controlling of reactive power from the grid [1]. Power flow solution for fixed speed wind turbine with induction generator was treated as P-Q bus [2]. The wind fluctuations in fixed speed topology are converted to mechanical fluctuations and consequently electrical power fluctuations [3].

For variable speed wind turbine, the generator is controlled by power electronic equipments. There are several reasons for preferring variable-speed wind turbines operation; among those are stresses reductions on the mechanical structure, acoustic noise reduction and the possibility to control both active and reactive power [4]. Most of wind turbine manufacturers are developing new larger wind turbines in the range of 3 to 10 MW [5]. These large wind turbines are all based on variable-speed operation with pitch control using direct driven synchronous generator (gearless) or doubly fed induction generator (DFIG) [6].

The major advantage of the variable speed wind energy conversion system with DFIG topology is that the power electronic components only have to handle a fraction (20-30%) of the total system power that leads to lower cost and size, while performing the same function of controlling voltage and frequency [7]. Analysis of the variable speed DFIG connected to the grid using rectifier-inverter converter in the rotor circuit was presented in [8]. The conventional induction machine equivalent circuit for computing the system steady state characteristics was presented in [9]. Balancing reactive power within the grid is one of the fundamental tasks. With increasing the penetration of wind power in power system, the wind power has to contribute in reactive power during both steady state and transient conditions [8].

In this paper, a mathematical model has been developed to evaluate the steady state performance of the variable speed wind energy conversion system with DFIG.

In addition a steady state converter (rectifier-inverter) model, as a function of the firing angles of the rectifier and inverter, is developed and used directly to calculate the influence of DFIG on operation of power system through power flow solution. These units are modeled as P-V bus(es) to manage the reactive power generation inside the wind farm. The paper presents and validates a model of DFIG suitable for operation in steady state operation and not only able to support voltage by feeding reactive power but also to fulfill the grid code requirement. The proposed algorithm is implemented and applied to the IEEE 26-bus system and the number of the equivalent WTGU at each generating bus is demonstrated and injected as P-V bus (es) to keep the reactive power margin planning of the test system in the planned margin. The impact of WTGUs on active and reactive power of its own generating bus and slack bus at different wind speeds are also investigated.

2. SYSTEM CONFIGURATION

The system in Figure 1 consists of a variable speed wind turbine with DFIG in which the stator is connected directly to the grid while the rotor winding is connected via a converter to the grid.

2.1Variable Speed Wind Turbine Modeling

The power output of the variable speed-pitch regulated wind turbine depends on the wind speed, rotor speed, both turbine and generator characteristics as well as the grid terminal voltage.

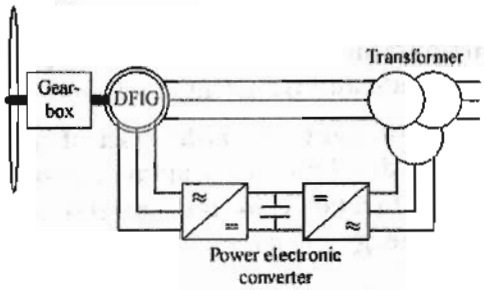

Fig. 1 DFIG Configuration System

For a given situation, wind speed is the only independent variable while the rotor speed and terminal voltage are dependent variables that vary with wind speed as well as the network conditions. In some of the existing models, either the turbine characteristics are neglected (constant mechanical power) or the WTGU power output is to be independent of the terminal voltage variation [9]. The method suggested here facilitates the computations of the exact power output of the WTGU without any simplifications. For the variable speed-pitch regulated wind turbine, the pitch angle controller regulates the wind turbine blade angle (β) according to the wind speed variations. Hence, the power output depends on the characteristics of the pitch controller in addition to the turbine and the generator characteristics.

The model is based on the steady state power characteristics of the turbine. The wind turbine mechanical power output is a function of rotor speed as well as wind speed and is expressed as: [10]

$$P_m(v_w,\omega_r)=\frac{1}{2}\rho A v_w^3 C_p(\lambda,\beta)$$

and $$\lambda=\frac{\omega_r R}{v_w} \qquad (1)$$

In a previous work the authors have developed a generic equation used to model $C_p(\lambda,\beta)$ [10]. The generic equation demonstrates optimum angular shaft speed (ω_r) and pitch angle (β) behavior versus wind speed variation, as illustrated in Appendix A.

2.2 DFIG Modeling

Modeling of DFIG includes equivalent circuit of the generator itself and the analysis of the rotor converter (rectifier – inverter) as follows.

2.2.1 Equivalent circuit

The equivalent circuit of the DFIG with inclusion of magnetizing losses is shown in Figure 2. This equivalent circuit is valid for steady state single phase model. Note that, if the rotor voltage V_r is short circuited the DFIG becomes ordinary squirrel cage induction generator.

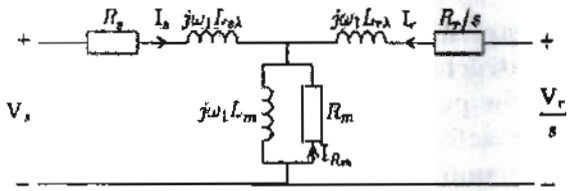

Fig. 2 Equivalent Circuit of the DFIG

Applying Kirchhoff's voltage law to the above circuit yields to [9]:

$$V_s = R_s I_s + j\omega_1 L_{s\lambda} I_s + j\omega_1 L_m (I_s + I_r + I_{Rm}) \qquad (2)$$

$$\frac{V_r}{S} = \frac{R_r}{S} I_r + j\omega_1 L_{r\lambda} I_r + j\omega_1 L_m (I_s + I_r + I_{Rm}) \qquad (3)$$

$$0 = R_m I_{Rm} + j\omega_1 L_m (I_s + I_r + I_{Rm}) \qquad (4)$$

The equations from (2) to (4) can be represented in the matrix form as:

$$\begin{bmatrix} V_s \\ \frac{V_r}{S} \\ 0 \end{bmatrix} = \begin{bmatrix} R_s + j\omega_1(L_m + L_{s\lambda}) & j\omega_1 L_m & j\omega_1 L_m \\ j\omega_1 L_m & \frac{R_s}{S} + j\omega_1(L_m + L_{s\lambda}) & j\omega_1 L_m \\ j\omega_1 L_m & j\omega_1 L_m & R_m + j\omega_1 L_m \end{bmatrix} \begin{bmatrix} I_s \\ I_r \\ I_{Rm} \end{bmatrix}$$

Where the slip S, is defined as:

$$S=\frac{\omega_1-\omega_r}{\omega_1} \qquad (5)$$

Moreover, if the air-gap flux, stator flux and rotor flux are defined as:

$$\Psi_m = L_m(I_s + I_r + I_{Rm}) \quad (6)$$

$$\Psi_s = L_{s\lambda} I_s + L_m(I_s + I_r + I_{Rm}) = L_{s\lambda} I_s + \Psi_m \quad (7)$$

$$\Psi_r = L_{r\lambda} I_r + L_m(I_s + I_r + I_{Rm}) = L_{r\lambda} I_r + \Psi_m \quad (8)$$

The equations from (4) to (6) can be rewritten as:

$$V_s = R_s I_s + j\omega_1 \Psi_s \quad (9)$$

$$\frac{V_r}{S} = \frac{R_r}{S} I_r + j\omega_1 \Psi_r \quad (10)$$

$$0 = R_m I_{Rm} + j\omega_1 \Psi_m \quad (11)$$

The resistive losses of the induction generator are

$$P_{Loss} = 3(R_s|I_s|^2 + R_r|I_r|^2 + R_m|I_m|^2) \quad (12)$$

and it is possible to express the electro-mechanical torque T_e, as:

$$T_e = 3n_p \operatorname{Im}[\Psi_m I_r^*] = 3n_p \operatorname{Im}[\Psi_r I_r^*] \quad (13)$$

Where n_p is the number of pole pairs.

2.2.2 Power flow of DFIG

In order to investigate the power flow of the DFIG, the apparent power fed to the DFIG via the stator and rotor has to be determined. The stator apparent power S_s and rotor apparent power S_r can be found as [9]:

$$S_S = 3V_s I_s^* = 3R_s|I_s|^2 + j3\omega_1 L_{s\lambda}|I_s|^2 + j3\omega_1 \Psi_m I_s^* \quad (14)$$

$$S_r = 3V_r I_r^* = 3R_r|I_r|^2 + j3\omega_1 S L_{r\lambda}|I_r|^2 + j3\omega_1 S \Psi_m I_r^* \quad (15)$$

By substituting I_s from equation (6) Equation (14) can be rewritten as following

$$S_S = 3R_s|I_s|^2 + j3\omega_1 L_{s\lambda}|I_s|^2 + j3\omega_1 \frac{|\Psi_m|^2}{L_m} + 3R_m|I_{Rm}|^2 - j3\omega_1 \Psi_m I_r^* \quad (16)$$

While equation (15) is still unchanged:

Now the stator and rotor active and reactive power can be determined as:

$$P_S = \operatorname{Re}[S_S] = 3R_s|I_s|^2 + 3R_m|I_{Rm}|^2 + 3\omega_1 \operatorname{Im}[\Psi_m I_r^*] \approx 3\omega_1 \operatorname{Im}[\Psi_m I_r^*] \quad (17)$$

$$P_r = \operatorname{Re}[S_r] = 3R_r|I_r|^2 - 3\omega_1 S \operatorname{Im}[\Psi_m I_r^*] \approx -3\omega_1 S \operatorname{Im}[\Psi_m I_r^*] \quad (18)$$

$$Q_S = \operatorname{Im}[S_S] = 3\omega_1 L_{s\lambda}|I_s|^2 + 3\omega_1 \operatorname{Re}[\Psi_m I_r^*] \quad (19)$$

(19)

$$Q_r = \operatorname{Im}[S_r] = 3\omega_1 S L_{r\lambda}|I_r|^2 + 3\omega_1 S \operatorname{Re}[\Psi_m I_r^*] \quad (20)$$

Neglecting the resistive and magnetizing losses leads to that the mechanical power produced by the DFIG can be determined as the sum of the stator and rotor power as follows:

$$P_{mech} = 3\omega_1 \operatorname{Im}[\Psi_m I_r^*] - 3\omega_1 S \operatorname{Im}[\Psi_m I_r^*] = 3\omega_r \operatorname{Im}[\Psi_m I_r^*] \quad (21)$$

Then, by dividing P_{mech} with mechanical rotor speed, $\omega_m = \omega_r/n_p$, the produced electromechanical torque, as given in eq. 13, can be found.

2.2.3 Steady state Model of DFIG Converters

The basic model is shown in Figure 3. On the AC side, the link is represented by two nodes r and i, whose voltages are $V_r \angle \theta_r$ and $V_i \angle \theta_i$, respectively. The AC currents at the rectifier and inverter terminals are denoted by $I_r \angle \varphi_r$ and $I_i \angle \varphi_i$, respectively. The line voltage on the secondary sides of the rectifier transformer is ($a_r V_r$) and the line current (I_r/a_r).

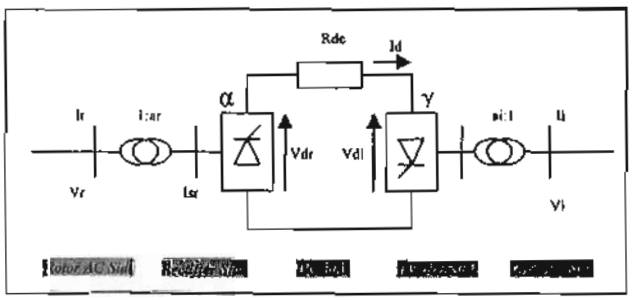

Fig.3. Single line Diagram of DFIG Converter

The direct voltage at the rectifier terminal V_{dr} is given as [11] :

$$V_{dr} = (3\sqrt{2}/\pi)(a_r V_r)\cos\alpha_r - 3(X_{cr}/\pi) I_d \quad (22)$$

Here α_r is the rectifier delay angle.The direct current I_d is related to the secondary AC line current by the following relations:

$$I_{sr} = (\sqrt{6}/\pi) I_d \qquad \text{But,} \quad I_{sr} = (I_r / a_r)$$

Then $I_r = a_r (\sqrt{6}/\pi) I_d$

Applying of KVL in DC link yields:

$$V_{dr} - V_{di} = I_d R_{dc} \tag{23}$$

Inverter voltage equation is given as [11]:

$$V_{di} = (3\sqrt{2}/\pi)(a_i V_i)\cos\gamma_i - 3(X_{ci}/\pi) I_d \tag{24}$$

Here γ_i is the inverter extinction angle.

The power relations are given by:

$$V_{dr} I_d = \sqrt{3} V_r I_r \cos\phi_r \tag{25}$$

$$V_{di} I_d = \sqrt{3} V_i I_i \cos\phi_i \tag{26}$$

AC line current of the inverter side is:

$$I_i = a_i (\sqrt{6}/\pi) I_d \tag{27}$$

3. The proposed Algorithm

A new algorithm has been developed to incorporate the variable speed wind turbine with doubly- fed induction generator through ac-dc-ac converter to study power flow analysis. The number of equivalent WTGUs at each generating bus was demonstrated. The main steps of the developed algorithm are:

1. Input:
   a. System data (bus data, line data, load data, and generation data),
   b. Wind turbine characteristics (cut-in speed, rated speed, cut-off speed, and rated power).
   c. DFIG parameters (Stator, Rotor and magnetizing resistances and reactances), number of poles, frequency, rated power, rated voltage and rated speed,
   d. Converter parameters (dc resistance, rectifier commutating, reactance inverter commutating reactance and off nominal tap changer for rectifier and inverter).
2. Compute slip then determine stator and rotor active power and plot slip versus wind speed.
3. Through variation of firing angle of the inverter and rectifier, rotor voltage can be controlled and rotor reactive power can be limited through margin.
4. From equivalent circuit of DFIG, compute magnetizing air gap voltage and current then determine stator voltage and current, and then get the stator, rotor and total power factor
5. Compute stator and rotor active power at each wind speed then compute mechanical power, stator and rotor reactive power limits as a function of both firing angles of rectifier and inverter at each wind speed.
6. Perform power flow analysis for the test system and check active and reactive power of the generating bus(es) and also the slack bus without WTGU.
7. Inject wind power at released generating bus(es) knowing (P & Q calculated as margin) of the test system by replacing of the selected bus.
8. Calculate active and reactive power (uncontrolled) of the selected bus and also the active and reactive power of slack bus at different wind speed.
9. Compute difference in active power (Δp) and reactive power (Δq) of the slack bus with and without WTGU at different wind speed (Δp and Δq).
10. End

4. Case Study

The proposed model is applied on IEEE-26 Test Bus System for studying the impact of variable speed wind turbine coupled with DFIG on the steady state power system operation.

4.1. DFIG Performance

The data and parameters of the DFIG that used in this paper are stated in the appendix (Tables A2-A4). Due to variation of shaft angular speed the slip

can be computed from Equation (5) and plotted at each wind speed as shown in Fig. 4. Then stator and rotor active power at each wind speed were calculated and summed up to generate the active power curve as shown in Fig. 5. Both of the stator and rotor power are derived as follows:

$P_s = P_{mech} / (1-S)$ and

$P_r = -S * P_{mech} / (1-S)$.

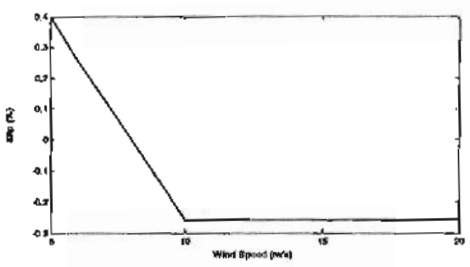

Fig.4 Slip as a Function of Wind Speed

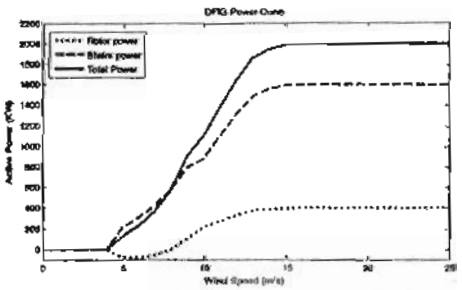

Fig.5. Characteristic of Power Curve for DFIG

The shares of the stator and the rotor in the generated power were represented in Table 1.

The DFIG feeds its electrical outputs (stator and rotor) into infinite bus-bar via static power ac-dc–ac converter in the rotor circuit through the variation of the firing angles (α) (0-20^0)&(γ) (10-30^0) of both rectifier and inverter respectively. Knowing active power of the rotor (P_r) and holding inverter terminal voltage (V_i) constant at 1 p.u., the reactive power output of the inverter (Q_r) and the input voltage of the rectifier (V_r) can be calculated as a function of firing angles (α)&(γ) using the Equations (22-27) as shown in Table 2.

4.2. IEEE-26 Bus System

The IEEE- 26 bus system is shown in Figure 6. The system consists of 6 generating buses and 20 load buses, total active power generation excluding the slack bus of the system is 719 MW. The total load of the entire system equals 1278.4 MW and 621.38 MVar, the base power of the system is taken as 100 MVA

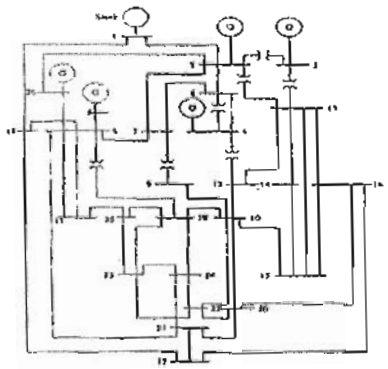

Fig. 6. Original IEEE-26 Bus System

and the total compensation reactive power is 22 MVar. The system has 7 transformers and 46 transmission lines. Bus 1 is considered as the slack bus [11]. The complete data of the system was given in [12].

4.3. Injection of Wind Farm into IEEE-26 Bus System at Bus #2

The wind farm consists of number of WTGUs depends on the injection bus capability. The units are taken as Vestas type (V80-2000) variable speed-pitch regulated coupled with doubly fed induction generator [13].

The effect of inserting WTGUs on the slack bus is measured using the Δp and Δq, where Δp and Δq are the per unit differences in active and reactive power as presented in Equation (28), respectively for the slack bus with wind turbines and the original test system at different wind speed.

$$\Delta P = \frac{P - P_{org}}{P_{org}}, \quad \Delta Q = \frac{Q - Q_{org}}{Q_{org}} \qquad (28)$$

The higher the value of Δp or Δq means that the slack bus is loaded more due to replacing the original generator with WTGUs

Power flow analysis for the *IEEE-26 Bus* system was performed while monitoring the status at the injection point (Bus #2) as shown in Table 3.

As shown from Table 3, the active power generated from the generator 2 is 79 MW. So, injecting 40 wind turbine units each 2MW as a replacement of generator 2 at Bus #2 in the system as P-V bus (P & Q calculated as margin) was performed. The change in active and reactive power of the slack bus including WTGUs from the base case of the system without wind were calculated and listed at different wind speed as shown in Table 4.

Here, the reactive power of the slack bus was affected extremely, especially at low wind speed. The reactive power calculated (Q_{cal}) may be negative, especially at low wind speed. This means that the WTGUs consume reactive power at this situation. However, this is illogical for generating buses. Here, there are two options to solve this lack of reactive power. Either solve it by reactive support or Flexible AC Transmission systems (FACTs), or even substitute this reactive power from neighbor generators.

4.4. Selection of WTGUs' Injection Bus

The possible injection buses are the generator buses in the system. It is obvious to say that, some buses could be better locations than others. This good injection bus in this selective criterion as designed is the bus that has low effect on the slack bus in terms of Δp and Δq as well as the active and reactive power injected at its own bus. The proposed algorithm is applied on the IEEE 26-bus system after injection of WTGU at each generating bus individually to investigate the site effect buses for three wind speed 5,10, and 16m/s as shown in Table 5.

As shown from Table 5, connecting WTGUs at certain generating buses such as buses 2, 3 and 4, the reactive power injected has negative values at different wind speeds meaning that the WTGUs consume reactive power from the system. So, this WTGUs injection has very bad effect on the slack bus. The effect on the slack bus is measured using Δq. The higher the value of "Δq", the more the reactive power requirement from the slack bus. This may lead to force the slack bus out of its reactive power limit. However, the good thing is that there are two buses namely; bus 5 and bus 26 almost don't have bad effect on the slack bus concluding that bus 5 and 26 are preferable sites. More precisely, bus 5 is the best location for injecting the WTGUs. Anyway, even injecting WTGUs at sites such as bus 2, 3 or 4 could be adjusted by reactive support or FACTs.

5. Conclusion

In this paper, a mathematical model has been developed to evaluate the steady state performance of the wind turbine generator units interconnected with the utility grid through doubly fed induction generator. The proper equations of the DFIG and the converter were used directly to calculate the performance of the WTGUs. The developed algorithm also facilitated the computation of both active and reactive power output of the variable speed- pitch regulated wind turbine coupled with DFIG. The main steady state analysis that was performed is the power flow analysis in which these units are modeled as P-V bus(es).

The proposed algorithm was implemented and applied to the IEEE 26-bus system, and WTGU were injected at all possible generator buses. The effect of the WTGUs' injection was monitored by two criteria; the reactive power injected at its own bus and the correspondence of the system slack bus, all compared with base case of the test system without wind generation (conventional IEEE-26 Test Bus System). Based on these criteria the possible WTGUs sites were ranked and the best site was identified. The reactive power requirements problem could be solved by installing reactive support or FACTs.

Table 1: Power Curve Data

WindSpeed (m/s)	rpm	Slip S [%]	ω_r (p.u.)	P_s (kw)	P_r (kw)	P_{elect}	$P_{mech}(\alpha,\gamma)$ (MW)	
							min	max
16-25	19	-0.26	1.26	1600	400	2000	2.27	2.75
15	19	-0.26	1.26	1590.4	397.6	1988	2.23	2.71
14	19	-0.26	1.26	1556	389	1945	2.21	2.67
13	19	-0.26	1.26	1484	371	1855	1.97	2.35
12	19	-0.26	1.26	1306.4	326.6	1633	1.75	2.05
11	19	-0.26	1.26	1096	274	1370	1.51	1.77
10	19	-0.26	1.26	882.4	220.6	1103	1.23	1.46
9	17	-0.13	1.13	801.68	109.32	911	0.91	1.16
8	15	0	1	580	0	580	0.68	0.88
7	13	0.13	0.87	423.2	-55.2	368	0.39	0.45
6	11	0.26	0.74	305.1	-79.1	226	0.25	0.31
5	9	0.4	0.6	212.5	-84.5	128	0.13	0.16

Table 2: Current Flow through DFIG

Wind Speed (m/s)	rpm	Slip S [%]	Power Factor total		Q_s (kVar)		Q_r (kVar)		Q_t (kVar)	
			min	max	min	max	min	max	min	max
16-25	19	-0.26	0.86	0.97	520	1200	41	240	561	1440
15	19	-0.26	0.86	0.97	516	1186	38	234	551	1420
14	19	-0.26	0.85	0.97	510	1170	35	228	540	1390
13	19	-0.26	0.85	0.96	471	1077	31	193	502	1270
12	19	-0.26	0.85	0.96	430	980	26	160	456	1140
11	19	-0.26	0.84	0.96	362	824	22	108	384	932
10	19	-0.26	0.84	0.96	290	664	18	58	308	722
9	17	-0.13	0.83	0.95	241	552	11	44	252	596
8	15	0	0.82	0.94	190	436	0	0	190	436
7	13	0.13	0.82	0.94	140	320	-22	-46	94	274
6	11	0.26	0.81	0.93	105	204	-17	-37	88	167
5	9	0.4	0.80	0.93	70	160	-10.6	-21.2	59.4	138.8

Table 3. Status of Bus #2 for the IEEE 26 Bus System

Bus 2 without Wind units	Generation			Q_{cal} Mvar	Slack Bus	
	MW	Q_{min}	Q_{max}		P	Q
	79	40	250	122	719	229

Table 4. Status of Bus #2 and Slack Bus for the IEEE 26 Bus System Inserting WTGUs at Bus #2

v m/s	Q Margin cover all Wind speeds		$P_{cal}(2)$	$Q_{cal}(2)$	Slack Bus			
					P	Δp (p.u.)	Q	Δq (p.u.)
5	5	58	10	-149	789	0.1	439	0.91
10			44	-103	754	0.05	388	0.69
16			80	-35	719	0.0	267	0.17

Table 5: Impact of WTGUs Injected at Different Generating Buses of IEEE -26 System

Bus#	Test System without Wind (Base Case)				Injection of Wind Farm					Slack Bus Impact	
	P	Q_{min}	Q_{max}	Q_{cal}	v m/s	P	Q_{min}	Q_{max}	Q_{cal}	Δp p.u.	Δq p.u.
2	79	40	250	122	5	10	8	66	-149	0.1	0.91
					10	44			-103	.05	0.69
					16	80			-35	0.0	0.17
3	20	40	150	63	5	2.6	1.5	16.5	-212	0.11	1.2
					10	11			-190	0.06	1.0
					16	20			-160	0.	0.65
4	100	40	80	50	5	12.5	6.3	82.5	-119	0.12	0.73
					10	55			-82	0.06	0.57
					16	100			-28	0.0	0.32
5	300	40	160	124	5	20	20	250	58	0.4	0.16
					10	165			97	0.18	0.07
					16	300			124	0	0.05
26	60	15	50	30	5	4	4	50	9	0.08	0.05
					10	33			14.2	0.04	0
					16	60			32.6	0	0

List of Symbols

DFIG Doubly Fed Induction Generator.
WTGU Wind turbine generating units
P_m Mechanical power of the turbine (W)
C_p Turbine Performance coefficient
ρ Air density (kg/m^3)
A Rotor swept area (m^2)
v_w Wind speed (m/s)
λ Tip speed ratio,
β Blade pitch angle (deg)
ω_r Rotor angular speed (rpm)
V_s Stator voltage; (V)
V_r Rotor Voltage; (V)
R_s Stator resistance; (Ω)
R_r Rotor resistance; (Ω)
I_s Stator Current; (A)
$L_{s\lambda}$ Stator leakage reactance; (A)
I_r Rotor current; (A)
$L_{r\lambda}$ Rotor leakage reactance; (H)
L_m Magnetizing reactance; (H)
ω_1 Stator angular speed (rpm);
S Slip.
n_p Number of pole pairs
α_r Rectifier delay angle (rad)
γ_I Inverter extinction angle (rad)
a_r , a_i rectifier and inverter tap ratio
x_{cr}, x_{ci} rectifier and inverter reactances
Q_{min}, Q_{max} Reactive Power Margin
Q_{cal} Calculated Reactive Power

6. References

[1] Slooteg J, Haan S, Polinder H, and Kling W, *Modeling Wind Turbines in Power System Dynamic Simulations*, IEEE Transactions on Power Systems Vol. 7, 2002, pp. 638-647.

[2] Petru T, *Modeling Of Wind Turbine for Power System Studies*, Ph.D. Thesis, Department of Electrical Power Engineering, Chalmers University of Technology, Sweden 2003.

[3] Petru T, and Thornier T, *Modeling ofWind Turbines for Power System Studies*, IEEE Transactions on Power Systems Vol. 4 No. 2, 2002, pp. 1132-1139.

[4] Sorensen P, Hancen A, Janosi L, and Bak-Jensen B, *Simulation of Interaction between Wind Farm and Power System*, Riso-R-1281(EN), Riso National Laboratory, Roskilde, December 2001.

[5] Ranngnathan V, and Datta R, *Variable Speed Wind Power Generation Using Doubly Fed Wound Rotor Induction Machine*, IEEE Transactions on Energy Conversion, Vol. 17 No. 3 September 2002.

[6] Slootweg J, Polinder H, and Kling W, *Dynamic Modeling of A Wind Turbine with Doubly Fed Induction Generator, IEEE Transactions on Electrical Power Systems*, Vol. 11 No. 2, March 2001.

[7] Ackermann T, *Wind Power in Power Systems*; John Wiley & Sons Ltd, Royal Institute of Technology, Stockholm, Sweden, 2005.

[8] Wilchand M, Pappala V, Erlich I, and Singh S, *Reactive Power Generation by DFIG Based Wind Farms with AC Grid Connection.* IEEE Power Tech., Lausanne 2007, Issue , 1-5 July 2007, pp. 626 – 632

[9] Petrson A, *Analysis, Modeling and Control of Doubly Fed Induction Generators for Wind Turbines.* PhD Thesis, Chalmers University, 2005.

[10] El-Saadawi M, Kaddah S, Osman M, and Abdel-Wahab M, *Impact of Wind Farms on Contingent Power System Voltage Stability,* The 12th International Middle-East Power Systems Conference, EPCON'2008, South Valley University, Aswan, Egypt, March 12-15, 2008.

[11] El-Sadek M. Z., *Power Systems Voltage Stability and Power Quality*, Mukhtar Press, Egypt, 2003.

[12] Saadat H, *Power System Analysis*; 2nd Edition McGraw Hill: WCB, 2002.

[13] "*Vestas Wind Systems: General Specification*", available on line at: www.vestas.com

Appendix

Wind Turbine Characteristics:

The performance coefficient C_p is given as [7]:

$$C_p(\lambda,\beta) = C_1\left(\frac{C_2}{\lambda_i} - C_3\beta - C_4\beta^{C_5} - C_6\right)e^{\frac{-C_7}{\lambda_i}} \quad (29)$$

Where

$$\frac{1}{\lambda_i} = \frac{1}{\lambda + C_8\beta} - \frac{C_9}{\beta^3 + 1}$$

C_1, C_2,.., C_9 are constant parameters of wind turbine shown in Table A1 :

Table A1 Constants of Variable Speed Wind Turbine Coefficient

C_1	C_2	C_3	C_4	C_5	C_6	C_7	C_8	C_9
0.73	151	0.58	0.002	2.14	13.2	18.4	-0.02	-0.003

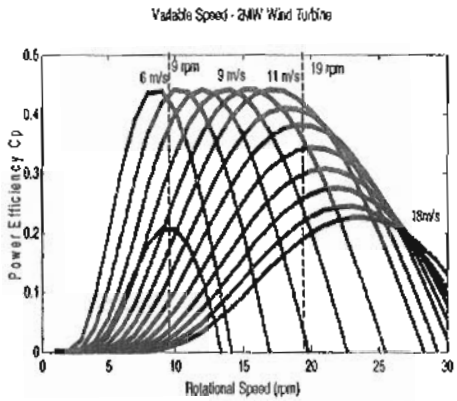

Fig. A1. Shaft Angular Speed versus Performance Coefficient

The nominal values of the DFIG are listed in Table A2 which are the base values of the per unit parameters of the generator presented in Table A3 which are used in equivalent circuit of DFIG

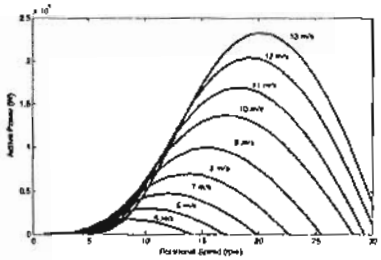

Fig. A2 Variable Speed Wind Turbine Power Characteristics

Using equation (29), Fig. A1 can be plotted which demonstrates shaft angular speed (ω) versus performance coefficient C_p at each wind speed (v), the limits of the angular speed (ω) as seen between 9 and 19 rpm which match nominal power of the generator.

The maximum shaft angular speed (ω) was tracked to get the maximum power till nominal power of the generator reached then (ω) has be fixed and pitch angle of the blade (β) should varied to keep the nominal power of the generator constant as shown in Figures A2, A3.

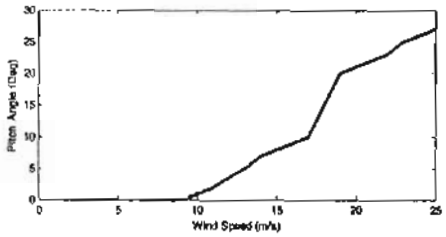

Fig. A3 Pitch Angle Characteristics

Table A2. Nominal Values of Wind Turbine DFIG

Wind Turbine Power Capacity	KW	2000
Wind Turbine Diameter	m	75
Rotor Swept Area A	m^2	4418
Gear Box Ratio		1:100
Low Shaft Speed Margin	rpm	9-18
Base Voltage (Phase-neutral)	$V_{n,P\rightarrow P}$	400 V
Base Current	I_b	1900 A
Base Frequency	f_b	314 rad/s
Base Impedance $Z_b = V_b / I_b$	Ω_p	0.21Ω

Table A3. Base and P.U. Values of the DFIG [8]

Stator Resistance	R_s	0.0022 Ω	↔	0.01 p.u.
Rotor Resistance	R_r	0.0018 Ω	↔	0.009 p.u.
Sintor Leakage Inductance	L_s	0.12 mH	↔	0.18 p.u.
Rotor Leakage Inductance	L_r	0.05 mH	↔	0.07 p.u.
Magnetizing Resistance	R_m	42 Ω	↔	198 p.u.
Magnetizing Inductance	L_m	3.1 mH	↔	4.4 p.u.